Supporting Information

High-Performance Overall Water Splitting Electrocatalysts Derived from Cobalt-Based Metal-Organic Frameworks

Bo You,[†] Nan Jiang,[†] Meili Sheng,[†] Sheraz Gul,[‡] Junko Yano,[‡] and Yujie Sun*[†]

[†]Department of Chemistry and Biochemistry, Utah State University, Logan, Utah 84322, USA;

[‡]Physical Biosciences Division, Lawrence Berkeley National Laboratory, Berkeley, California 94720, USA

E-mail: yujie.sun@usu.edu; *Fax: +1-435-797-3390; Tel: +1-435-797-7608*

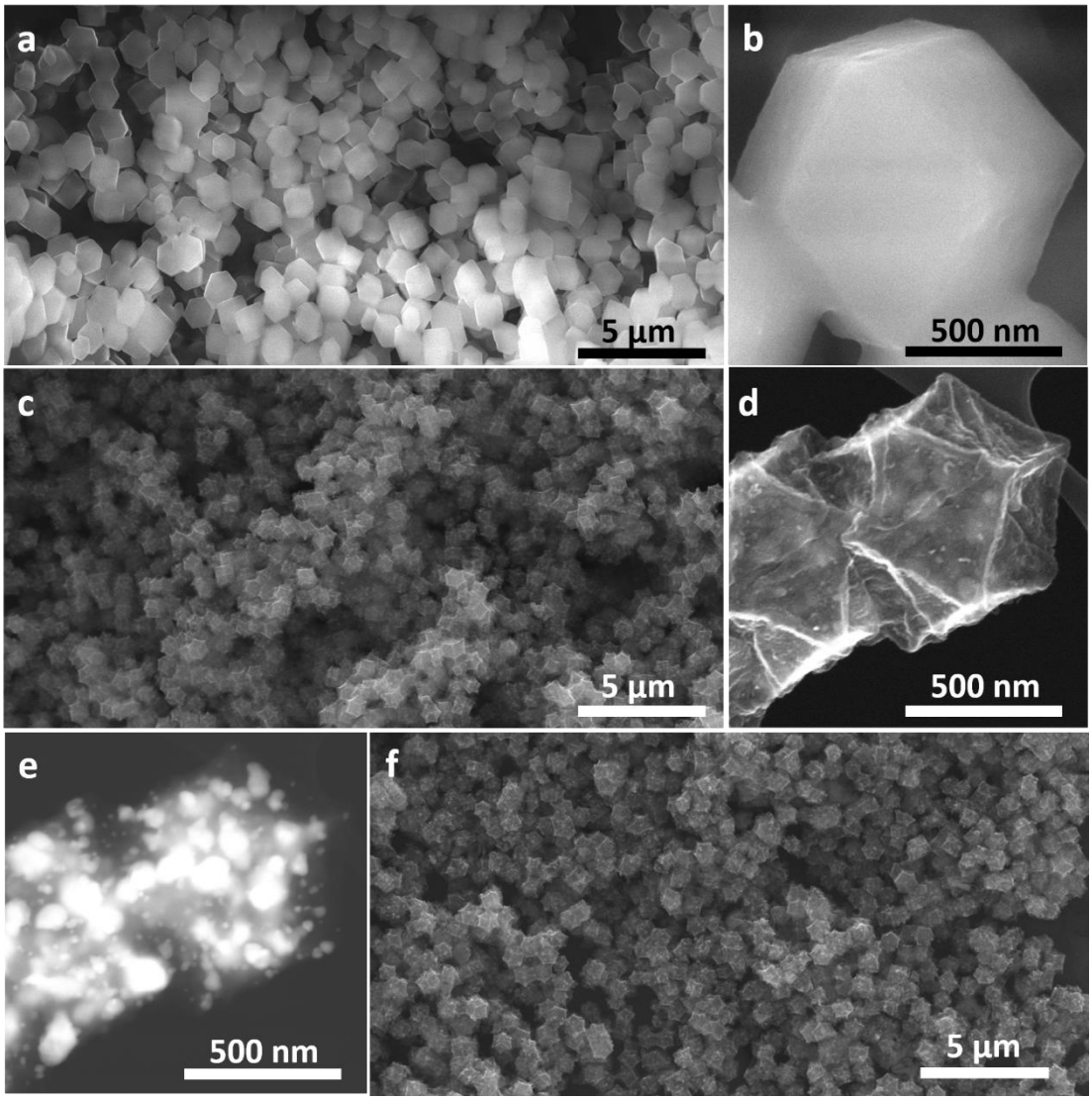

Figure S1 (a, b) SEM images of ZIF-67, (c, d) SEM images of Co/NC-900, (e) TEM images of Co/NC-900 shown in (d). (f) SEM image of Co-P/N-C-900-2 (*denote as Co-P/NC in the main text for brevity*).

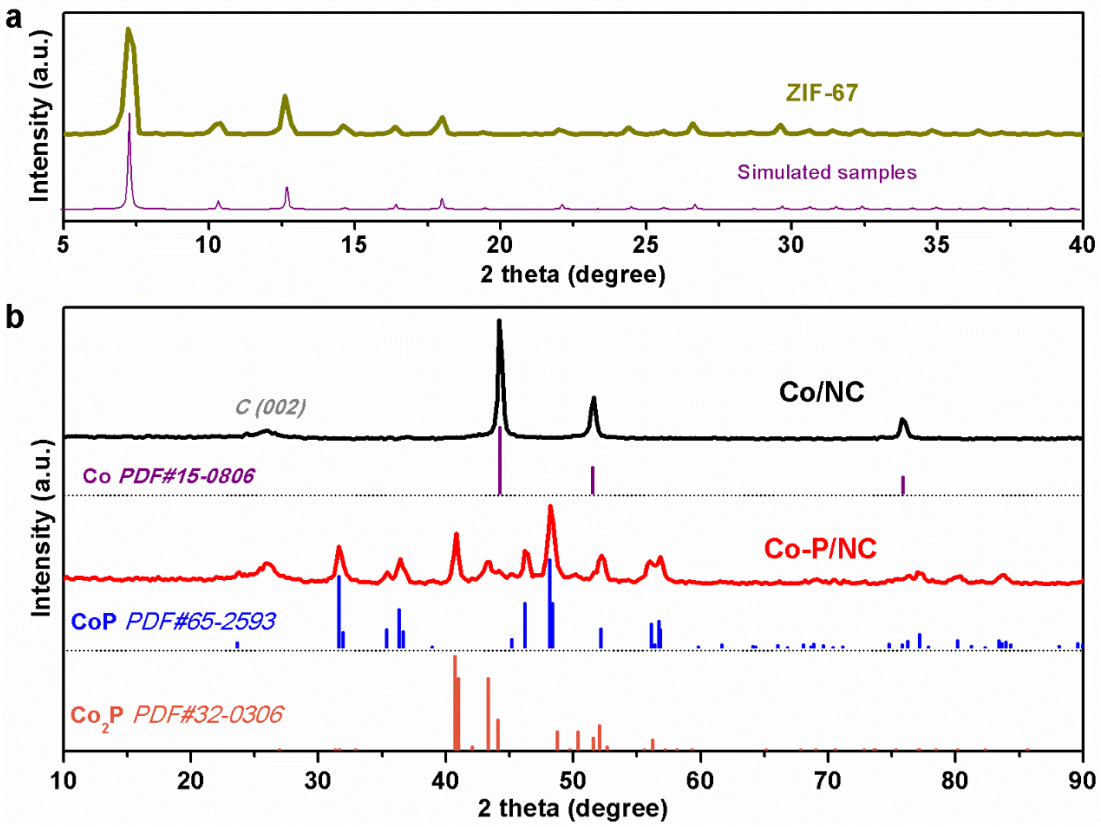

Figure S2 XRD patterns of (a) ZIF-67 and the simulated samples, and (b) the resulting Co/NC, Co-P/NC, and the XRD standard patterns of Co, CoP, and Co_2P.

The peaks at 2 theta of 40.8° and 46.2° were used to estimate the crystallite sizes of Co_2P and CoP via the standard Debye-Scherrer formula, respectively. The calculated sizes are ~33 nm for both Co_2P and CoP.

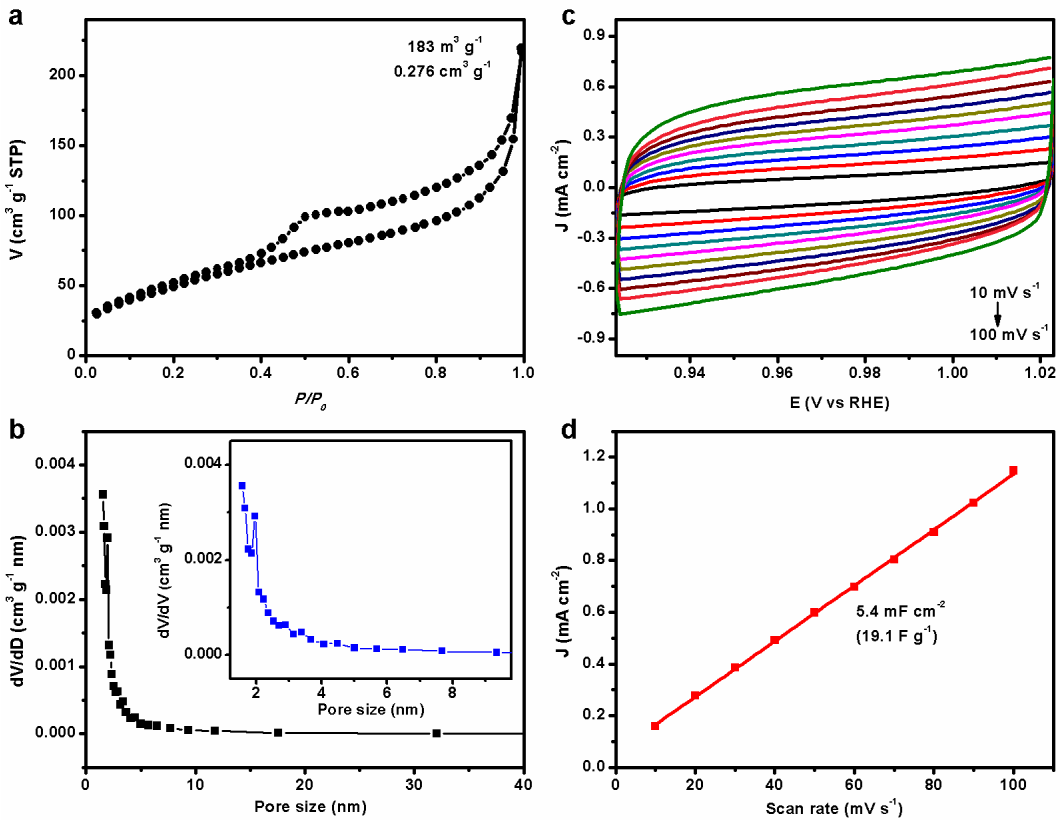

Figure S3 (a) N_2 sorption isotherms and (b) the corresponding pore size distribution curves of Co-P/NC. The inset shows the expanded region of the small pore size. (c) Cyclic voltammograms curves of Co-P/NC at the scan rates ranging from 10 to 100 mV s^{-1}. (d) Scan rate dependence of the current density difference of the cathodic and anodic scans at 0.973 V vs RHE of Co-P/NC.

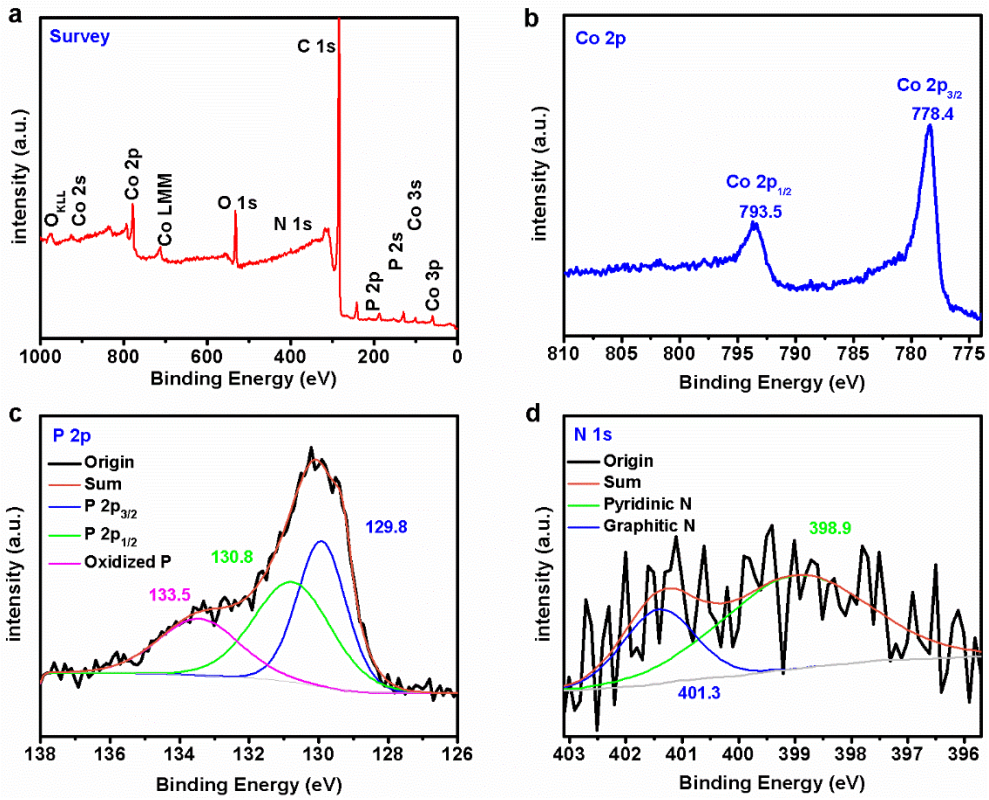

Figure S4 XPS spectra for the (a) survey scan, (b) Co 2p region, (c) P 2p region, (d) N 1s region of Co-P/NC.

The X-ray photoelectron spectroscopy (XPS) showed that Co-P/NC consisted of C, Co, P, and N (Figure S4a, survey spectrum), in agreement with the element mapping results (Figure 1d in the main text). A detailed analysis of the Co 2p indicated the presence of two peaks at 793.5 and 778.4 eV (Figure S4b), assignable to Co $2p_{1/2}$ and Co $2p_{3/2}$, respectively. A high-resolution image of the P 2p (Figure S4c) region shows two peaks at 130.8 and 129.8 eV, reflecting the binding energy (BE) of P $2p_{1/2}$ and P $2p_{3/2}$, respectively, along with one peak at 133.5 eV. The peak at 133.5 eV is assigned to oxidized phosphorus species, which arise from superficial oxidation because of air contact (*J. Catal*. **2005**, *231*, 300; *Angew. Chem*. **2014**, *126*, 6828). The survey spectrum (Figure S4a) also confirms the existence of O in the Co-P/NC sample. The peaks at 778.4 and 129.8 eV are close to the binding energies (BEs) for Co and P in CoP or Co_2P (*Nano Energy* **2014**, *9*, 373; *J. Am. Chem. Soc*. **2014**, *136*, 7587.; *Chem. Mater*. **2008**, *20*, 7081). The Co 2p BE of 778.4 eV is positively shifted from that of metallic Co metal (777.9 eV), and the P 2p BE of 129.8 eV is negatively shifted from that of elemental P (130.2 eV) (*Practical Surface Analysis by Auger and X-ray Photoelectron Spectroscopy*, John Wiley & Sons: New York, 1983.). It suggests the Co in Co-P/NC has a partial positive charge (δ^+) while the P has a partial negative charge (δ^-), implying transfer of electron density from Co to P which is consistent with previous calculations and electron density maps (*Inorg. Chem*. **2005**, *44*, 8988.). High resolution N 1s spectra (Figure S4d) can be deconvoluted into mainly two peaks of graphitic N (401.3 eV) and pyridinic N (398.9 eV) (*ACS Nano* **2011**, *5*, 4350.).

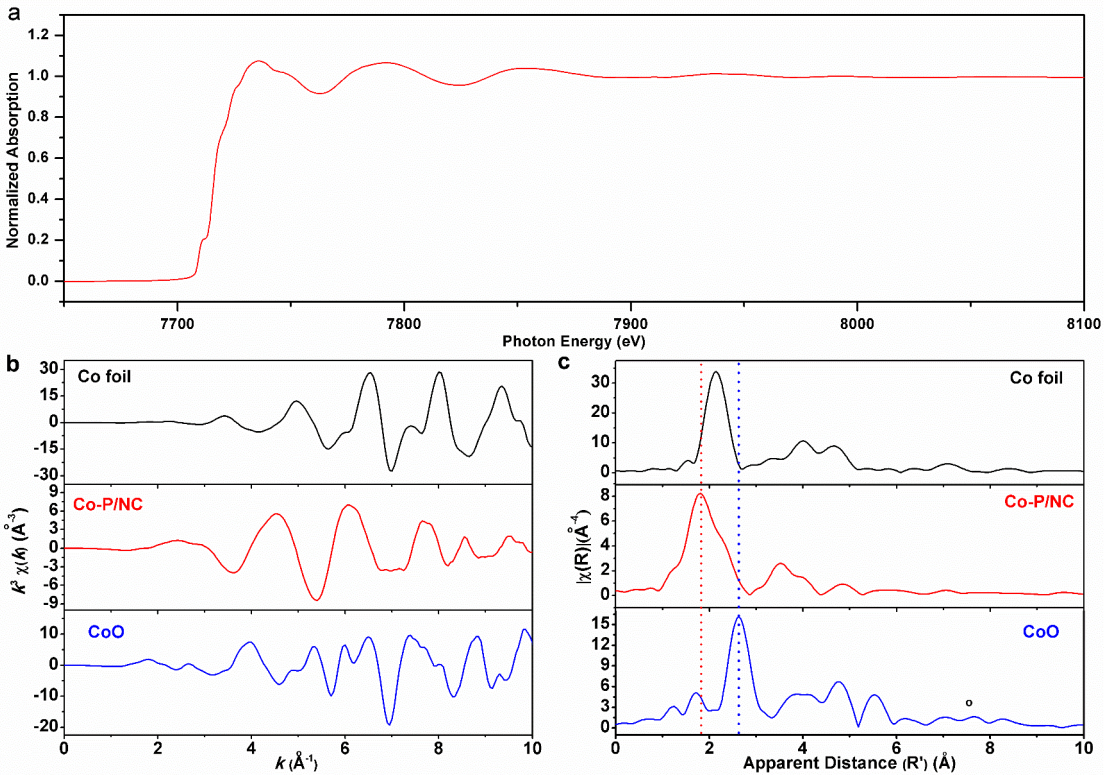

Figure S5 (a) Co K-edge X-ray absorption spectrum of Co-P/NC which is very close to the reported spectrum of CoP_x (*J. Mater. Chem.* **2011**, *21*, 11498.). (b and c) Co K-edge EXAFS spectra (in k-space and r-space, respectively) of Co foil, CoO, and Co-P/NC.

Table S1 EXAFS fitting parameters corresponding to the fit in Figure 2b.

Path	**Coordination Number**	**R (Å)**	**ΔE_0 (eV)**	**σ^2 (Å^2)**
Co-P	3.7 ±0.4	2.24 ±0.01	–3.019 ±1.658	0.0075 ±0.001
Co-Co	6.6 ±0.6	2.60 ±0.01	–3.019 ±1.658	0.015 ±0.002

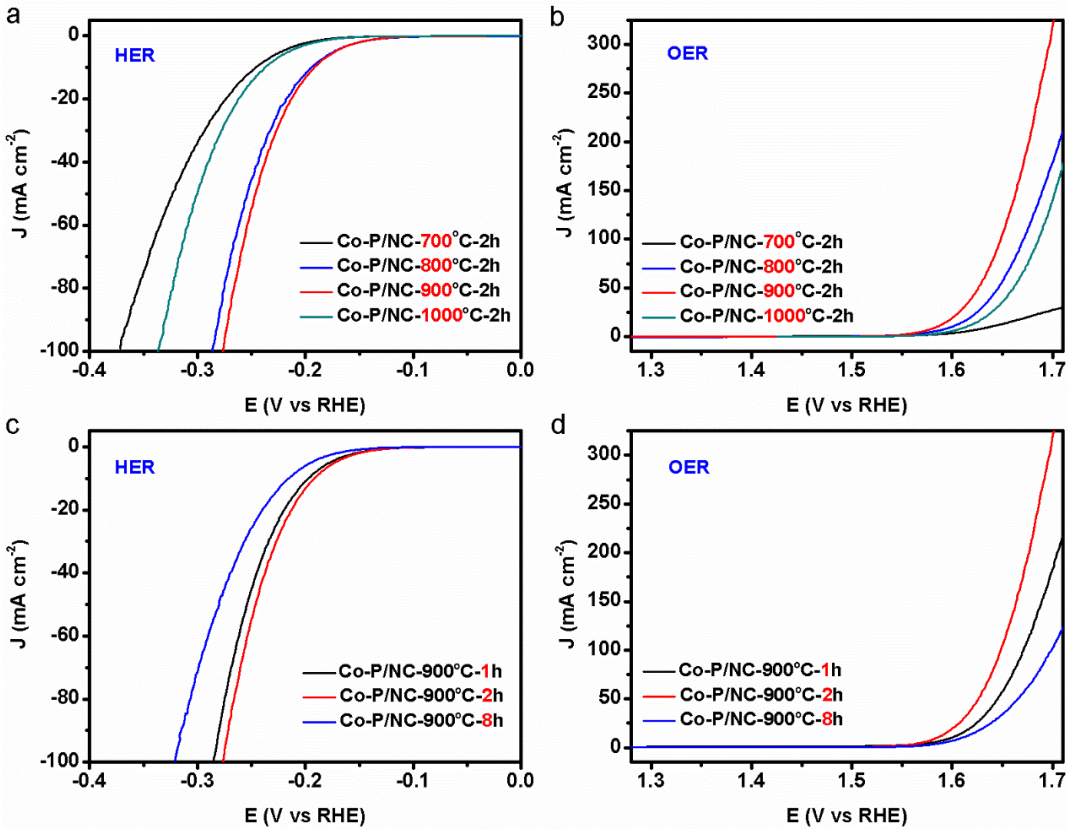

Figure S6 RDE polarization plots (a, c for HER and b, d for OER) measured with Co-P/NC-x-y samples in 1.0 M KOH electrolyte at 2000 rpm and 2 mV s^{-1} as a function of (a, b) the carbonization temperature and (c, d) the phosphidation time.

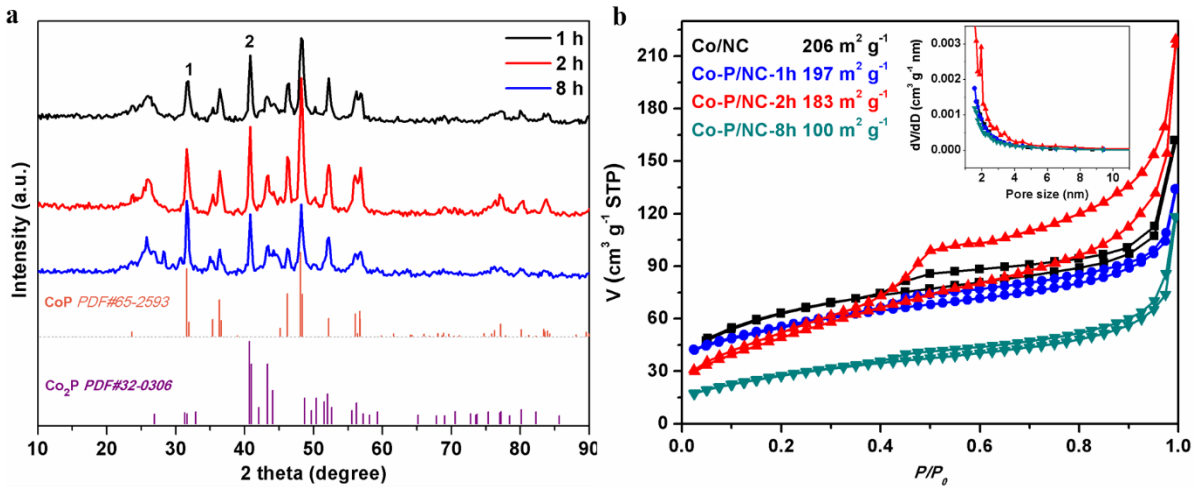

Figure S7 (a) XRD patterns and (b) N_2 sorption isotherms of Co-P/NC-y samples. The inset in (b) are the corresponding pore size distribution curves.

As shown in the XRD patterns (Figure S7a), the intensity ratio of peak 1 at 2 theta of 31.6° and peak 2 at 2 theta of 40.8° can be used to roughly estimate the ratio of CoP over Co_2P. When the phosphidation time increased from 1 h to 2 h, the intensity ratio of peak 1 over peak 2 increased from 0.586 to 1.248, indicating the increased content of CoP. Further prolonging phosphidation time to 8 h resulted in the intensity ratio of peak 1 over peak 2 increasing to 1.304. Although a recent report has showed that CoP possesses higher HER activity in acidic media than the morphologically equivalent Co_2P (*Chem. Mater.* **2015**, *27*, 3769.), in our case the long-time phosphidation would result in low specific surface area of the resulting materials. For example, after carbonization, the resulting Co/NC (prior to phosphidation) exhibited a specific surface area of 206 m^2 g^{-1}; while after phosphidation for 1, 2, and 8 h, the specific surface areas of the corresponding materials (Co-P/NC-1 h, Co-P/NC-2 h and Co-P/NC-8 h decreased from 197, 183, to 100 m^2 g^{-1} (Figure S7b). Overall, the best HER and OER activity was achieved with phosphidation for 2 h, as revealed by the HER and OER polarization plots (Figure S6), probably because an optimal balance of specific surface area, catalyst composition, active site density, and electron conductivity was realized under this synthetic condition. Considering our primary pursuit was to develop a highly active non-precious water splitting catalyst and following the common procedures in recent literature (*Angew. Chem. Int. Ed.* **2015**, 54, 8188; *Angew. Chem. Int. Ed.* **2014**, 53, 9577; *Chem. Mater.* **2015**, 27, 2026.), we therefore took the optimal parameters to prepare Co-P/NC catalysts for further electrochemical characterizations in the main text.

Table S2 Comparison of electrocatalytic HER activity of various nonprecious catalysts in 1.0 M KOH electrolyte.

Catalysts	Loading (mg cm^{-2})	S_{BET} (m^2 g^{-1})	J (mA cm^{-2})	η (mV)	Tafel slop (mV dec^{-1})	Mass activity (A g_{metal}^{-1})[a]	Reference
Co-P/NC	**0.283**	**183**	**10** **20** **100**	**-191** **-212** **-277**	**51**	**365.1**	**This work**
	1.0		**10** **20** **100**	**-154** **-173** **-234**	**-**	**337.2**	
NiFe LDH/Ni foam	-	-	10 20	>-200 ~-250	-	-	*Science* **2014**, 345, 1593.
Co-P film	2.52 (Co)	-	10 20	94 115	42	~200	*Angew. Chem. Int. Ed*. **2015**, 54, 6251.
MoC_x/C	0.8	147	10 20	-151 >-175	59	-	*Nat. Commun.* **2015**, 6, 6512.
CoO_x@CN	0.42	-	10	-232	N/A	-	*J. Am. Chem. Soc*. **2015**, 137, 2688.
MoS_{2+x}/FTO	-	-	10	-310	N/A	-	*Angew. Chem. Int. Ed.* **2015**, 54, 664.
CoP/CC	0.92	36.5	10 100	-209 >-500	129	<16.6	*J. Am. Chem. Soc*. **2014**, *136*, 7587
Co-S/FTO	-	-	1	-480	N/A	<<12.6	*J. Am. Chem. Soc*. **2013**, 135, 17699.
Co-NRCNTs	~0.28	-	10 20	-370 >-450	N/A	<162	*Angew. Chem. Int. Ed*. **2014**, *53*, 4372.
Ni_2P	1.0	~32.8	20	-205	N/A	<25.3	*J. Am. Chem. Soc*. **2013**, 135, 9267.
MoB	2.3	-	10	>-225	N/A	<11.2	*Angew. Chem. Int. Ed*. **2012**, 51, 12703.
$Ni/Ni(OH)_2$	-	-	10	>-300	N/A	-	*Angew. Chem. Int. Ed.* **2012**, 51, 12495.
MoS_x	-	-	10	>-540	N/A	-	*Chem. Sci.* **2011**, 2, 1262.
FeP NAs/CC	~1.5	-	10	-218	146	~10.4	*ACS Catal.* **2014**, 4, 4065.
N, P-G	0.20	-	10	>-700	145	-	*ACS Nano* **2014**, 8, *5290*.
Ni_2P	0.38	-	20	-250	N/A	<33.3	*Phys. Chem. Chem. Phys.* **2014**, 16, 5917.

[a] Mass activity represents the current density that normalized by mass loading (A g^{-1}) at an overpotential of -200 mV.

Table S3 Comparison of electrocatalytic **OER** activity of various nonprecious catalysts in 1.0 M KOH electrolyte.

Catalysts	**Loading** ($mg\ cm^{-2}$)	S_{BET} ($m^2\ g^{-1}$)	**η (mV) at** 10 mA cm^{-2}	**Tafel slop** ($mV\ dec^{-1}$)	**Mass activity** ($A\ g_{metal}^{-1}$)[a]	**Reference**
Co-P/NC	**0.283**	**183**	**354**	**52**	**227.4**	**This work**
	1.0		**319**	**-**	**181.4**	
CoCo LDH	-	-	393	59		*Nat. Commun*. **2014**, 5, 4477.
NiCo-(b) Co/P-(a) Co/B Ni/B	-	-	420 380 >400 >400	N/A	-	*J. Am. Chem. Soc*. **2015**, 137, 4347.
CoO_x@CN	0.42	-	~385	N/A	-	*J. Am. Chem. Soc*. **2015**, 137, 2688.
Co-P films	2.52 (Co)	-	345	47	<10	*Angew. Chem. Int. Ed.* **2015**, 54, 6251.
$MnCo_2O_x$	0.142	-	>410	84	~88	*J. Am. Chem. Soc*. **2014**, 136, 16481.
$CoFeO_x$ film	-	-	~360	N/A	-	*J. Am. Chem. Soc*. **2013**, 135, 16977.
CoO_x film	-	-	403	42	-	*J. Am. Chem. Soc*. **2012**, 134, 17253.
$NiFeO_x$ film	-	-	>350	N/A	-	*J. Am. Chem. Soc*. **2013**, 135, 16977.
MnO_x film	-	-	563	49	-	*J. Am. Chem. Soc*. **2012**, 134, 17253.
Co_3O_4/N-rmGO	1.0	-	310	67	<100	*Nat. Mater.* **2011**, 10, 780.
$NiCoO_x$	-	-	>420	N/A	-	*J. Am. Chem. Soc.* **2013**, 135, 16977.
NiCo LDH	0.23		>420	62		*Nano Lett.* **2015**, 15, 1421.
N-G-CoO	0.7	25.31	340	71		*Energy Environ. Sci.* **2014**, 7, 609.
$Ni_xCo_{3-x}O_4$	2.3-2.7	112	~370	59~64	~8.6	*Adv. Mater.* **2010**, 22, 1926.

[a] Mass activity represent the current density that normalized by mass loading ($A\ g^{-1}$) at an overpotential of 350 mV.